Econ. Environ. Geol.
Vol. 29, No. 2, p. 171-182, 1996.

Geochemical Characteristics of the Quaternary Jungok Basalt in Choogaryong Rift Valley, Mid-Korean Peninsula

Soo-Meen Wee*

ABSTRACT : **Quaternary Jungok basalts are distributed along the old Hantan river in Mid-Korean Peninsula. They were flowed out from Mt. Ori and Upland (680 m), and they formed narrow and long basalt plateau showing the layers of 10 to 20 meters in thickness and about 95 km in length. Fifty seven samples were collected from the study area, and sixteen rock samples were selected and analysed for major and trace elements. The analyzed samples have alkalic composition and show a relatively restricted variation in major element chemistry (except MgO), as comparing to the that of trace element. Based on major element chemistry, a quantitative modelling of fractional crystallization by multiple linear regression method suggests that the chemical evolution of the evolved rocks can be generated by fractionation of olivine, plagioclase, clinopyroxene, and magnetite in proportion of 56 : 25 : 17 : 2, respectively. The calculated trace element abundances by mineral proportions estimated from major element modelling, however, underestimate the incompatible element concentrations in the evolved rocks. According to the incompatible element abundances, simple fractional crystallization process has difficulty to explain the chemical variation of the evolved rocks. It seems that the other processes, which enrichment of incompatible elements can occure without concomitant changes in major element compositions, are needed in order to explain the chemical variation of the Jungok basalts. Thus, the major elements and compatible trace elements variations of the Jungok basalts are due to fractional crystallization, but the incompatible elements variation is due to fractional crystallization superimposed on already varying concentrations caused by slightly different degrees of melting of the same source, and/or due to periodic replenishment, tapping and fractionation(RTF) processes.**

INTRODUCTION

Choogaryong rift valley, which located between Wonsan and Seoul in mid-Korean Peninsula trending in the direction of N15°E, is considered as a geotectonic rupturing in the time of post-Jurassic Deabo Orogeny. Three stages of volcanic activities are recognized in this area. Three volcanic activities are characterized by acidic volcanic rocks, tholeiitic basalts of Cretaceous age, and Quaternary Jungok basalts which distributed along the old Hantan river. Since the Jungok basalt is one of the Cenozoic alkaline suites of the Circum Japan Sea region and, it is very important to understand Quaternary volcanic activities in the Korean Peninsula. Thus, this investigation focussed on geochemistry of the Jungok basalt in the Choogaryong rift valley.

Many studies have been done to clarify petrographical characteristics of the volcanic rocks, and to understand tectonic episodes of this region (Takahashi, 1962; Lee, 1981; Lee *et al.*, 1983; Won, 1983; Kim *et al.*, 1984, Won *et al.*, 1990). However, geochemical studies of the Jungok basalts are a few and geochemical data are not enough to evaluate petrochemical evolution and magma source of the lavas. Thus, more data must be obtained in order to make reasonable petrogenetic interpretations of the Jungok basalts. Here, new mineral chemistry and whole rock chemical data are reported and dicussed

* Department of Earth Science Education, Korea National University of Education, Cheongwon-Kun, Chungbuk 363-791, Korea

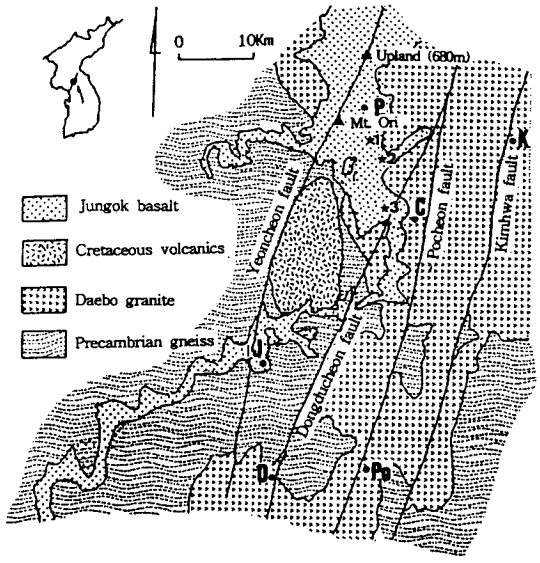

Fig. 1. Geologic map of the southern area of the Choogaryong rift valley (after Won *et al.*, 1990). 1~3; Sampling location (1; Co, 2; CH, 3; CB). J; Jungok, P; Pyeonggang, K; Kimhwa, C; Cheolwon, Po; Pocheon, D; Dongducheon.

in order to constrain the magmatic evolution of the Jungok basalts.

GENERAL GEOLOGY

The study area is composed of Precambrian basement gneiss, Jurassic granites, Cretaceous volcanics, and Quaternary basalts and unconsolidated sedimentary rocks as shown in Fig. 1. Jurassic Daebo granites intruded into the Precambrian basement rocks which are composed of banded gneiss, granitic gneiss and porphyroblastic gneiss. The Daebo granite is medium to coarse grained biotite granite which occured as batholith in the Choogaryong rift valley. According to the age dating by K-Ar method, the age of the Daebo granite is 165 Ma (Ueda, 1968).

Volcanic rocks in the study area are composed of Cretaceous acidic volcanic rocks, Cretaceous tholeiitic basalts, and Quaternary Jungok basalts. The Creataceous acidic volcanic rocks are distributed in the central part of the study area and consist of dacite, rhyolitic welded tuff, and tuff breccia. The tholeiitic basalts are occured as small outcrops in a very limited area. They are porphyritic and consist of plagioclase and clinopyroxene as dominant phenocryst phases, chlorite and serpentine occured as altered minerals (Lee *et al.*, 1983). The tholeiitic basalts commonly show flow structure and include cavities filled with calcite, quartz and zeolite. Quaternary Jungok basalts are distributed along the old Hantan river path delineated the vesicles curved toward down stream. Both numbers and thickness of lavas increase toward upstream direction. This fact suggests that the lava flowed from upstream side of the river (Kim *et al.*, 1984). The Jungok basalts were flowed out from Mt. Ori and Upland (680 meters high) and formed narrow and long basalt plateau showing the layers of 10 to 20 meters in thickness and about 95 km in length. These basaltic lavas were erupted more than eleven times comparatively in a short period (Won, 1983). According to the age dating by K-Ar method, the age of the uppermost basalt flow is 0.27 Ma and the volcanic activity had been continued to 0.1 Ma (Choi, 1982).

SAMPLING AND ANALYTICAL METHOD

Fifty seven samples were collected from the Quaternary Jungok basalts for petrological and geochemical study. Selected sixteen rock samples were analyzed for major and trace elements. Philips (PW-1480) X-ray fluorescense spectrometer was used to determine major element compositions of the whole rock. REE and selected trace elements were analyzed by Inductively Coupled Plasma mass-spectrometer (VG Elemental-PQ II Plus) at Korea Basic Science Center. Sample powders for analysis were prepared by grinding in a tungsten carbide shatter box. Major element compositions of olivine, pyroxene and plagioclase in selected samples were determined on the JEOL-733 electron microprobe at Korea University using 15 kv accelerating voltage, a 20 nA beam current and a 10 micron beam diameter. Sampling bias was avoided by selecting enough number of samples within the same rock units to encompass any small scale heterogenieties in rock compositions. Most of the samples were fresh and

Table 1. Representative mineral analyses from Jungok basalts.

	PLAGIOCLASE										
	CH-3		CO-1		CO-2		CO-3	CH-2		CB-31	
	mph	mph	mph	mph	mph	mph	ph	ph	mph	ph	mph
SiO_2	51.18	55.45	51.80	51.52	50.67	50.90	50.46	50.46	51.74	51.21	52.85
Al_2O_3	31.40	27.46	31.79	30.91	31.48	31.16	31.17	31.17	29.86	31.28	30.60
FeO	0.58	0.55	0.34	0.41	0.20	0.13	0.36	0.36	0.47	0.58	0.67
TiO_2	0.32	0.26	0.15	0.05	0.10	0.20	0.27	0.27	0.18	0.10	0.10
CaO	13.67	9.11	13.57	13.09	14.01	13.49	13.48	13.48	12.38	13.49	12.87
Na_2O	3.34	4.92	3.28	3.52	3.29	3.30	3.06	3.06	3.46	3.35	3.87
K_2O	0.39	0.94	0.20	0.25	0.22	0.29	0.45	0.45	0.40	0.35	0.41
Total	100.89	98.69	101.13	99.75	99.97	98.79	99.25	99.25	98.49	100.42	101.37
An%	69.30	50.60	69.60	67.20	70.20	65.90	70.90	70.90	66.40	69.00	64.80
	OLIVINE										
	CH-3		CO-1		CO-2		CB-31	CH-21		CB-21	CO-6
	mph	mph	ph	mph	ph	ph	ph	ph	mph	ph	mph
SiO_2	38.97	38.96	39.91	39.14	40.31	39.45	38.79	39.02	38.62	39.52	37.20
FeO	21.16	20.73	15.37	18.58	14.98	19.65	20.22	20.52	23.50	18.87	28.00
MgO	39.39	38.99	43.60	41.00	44.19	40.15	39.57	39.02	36.08	41.22	32.85
MnO	0.44	0.36	0.36	0.35	0.38	0.30	0.33	0.22	0.31	0.29	0.74
CaO	0.37	0.33	0.33	0.31	0.24	0.29	0.36	0.34	0.37	0.28	0.38
Na_2O	0.35	0.10	0.10	0.29	0.23	0.19	0.44	0.45	0.22	0.25	0.30
Total	100.68	99.67	99.67	99.67	100.23	100.03	99.71	99.57	99.10	100.43	100.47
F_0%	76.80	83.50	83.50	79.70	84.00	78.50	77.70	77.20	73.20	79.60	66.90
	PYROXENE										
	CH-3		CO-1	CO-2		CO-3	CB-31		CO-6	CH-1	CO-3
	mph	mph	mph	mph	ph	mph	ph	mph	mph	mph	mph
SiO_2	44.02	42.58	42.36	46.30	44.21	44.89	48.25	42.55	48.41	48.72	49.65
Al_2O_3	5.98	7,39	6.91	7.08	6.59	7.57	5.21	6.48	4.68	4.54	4.10
FeO	11.87	10.48	12.17	8.53	9.81	7.58	8.41	13.26	7.52	8.46	7.50
MgO	9.12	9.24	8.54	11.24	9.89	11.48	12.76	7.97	12.85	12.41	13.27
TiO_2	6.17	6,47	6.89	4.56	5.81	4.73	3.34	6.67	2.65	2.98	2.39
CaO	21.57	21.32	21.36	22.52	21.63	21.36	21.86	21.82	21.88	21.64	22.38
Na_2O	0.76	0.89	0.92	0.79	0.72	0.56	0.62	0.74	0.43	0.47	0.57
Total	100.49	98.37	99.15	101.02	98.66	98.17	100.45	99.81	98.42	99.22	99.90

ph; mineral grains which are greater than 0.5 mm in size,
mph; microphenocrysts with grain size range from 0.1 to 0.5 mm.

altered parts were avoided in order to enhance the accuracy of chemical data.

RESULTS

Petrography and Mineral Chemistry

The Jungok basalts have fairly uniform petrographic features, and consist predoninantly of plagioclase, olivine, clinopyroxene, and a variable amount of Fe-Ti oxides. Olivine and plagioclase are the major phenocryst phases in most of the samples, and clinopyroxene is also occured as phenocryst in some samples such as CO-2 and CB-31. Olivine phenocrysts often show spinel inclusions, and are partially replaced by iddingsite. Groundmass is composed of olivine, pyroxene, plagioclase, magnetite, and apatite. Ophitic texture which pyroxene surrounds plagioclase are often found. Plagioclase generally occurs as euhedral to subhedral grains and, in some cases, plagioclases show a well developed orientation.

Table 2. Major and trace element abundances of the Jungok basalts.

	CB-10	CB-12	CB-20	CB-21	CB-23	CB-29	CB-31	CH-1	CH-2	CH-3	CH-4	CO-1	CO-2	CO-3	CO-6	CO-7
SiO_2	48.67	47.73	47.80	48.55	47.82	48.47	47.99	47.99	47.99	47.32	48.21	46.84	48.53	48.20	48.13	48.15
TiO_2	1.92	1.90	2.00	1.87	1.90	1.83	1.83	2.13	1.83	1.78	1.60	2.06	1.91	1.91	1.59	1.79
Al_2O_3	15.68	15.50	15.83	15.35	15.78	15.55	15.51	15.37	15.56	14.80	15.45	16.47	15.62	15.44	15.12	16.66
FeO*	11.46	11.07	11.40	11.58	11.61	11.18	10.55	11.11	11.14	11.75	11.40	11.72	11.21	11.18	11.65	10.89
MnO	0.16	0.15	0.15	0.16	0.16	0.15	0.15	0.15	0.16	0.16	0.16	0.15	0.16	0.16	0.15	0.14
MgO	8.73	9.63	8.79	9.15	9.13	8.79	9.93	6.37	9.59	10.43	9.68	8.31	9.31	9.24	10.67	7.82
CaO	8.14	8.30	7.76	8.00	7.99	8.35	8.43	8.41	8.86	8.33	8.40	7.43	7.99	8.08	8.05	8.23
Na_2O	2.65	2.35	2.49	2.82	2.26	2.57	2.63	2.59	2.07	2.31	2.49	2.15	2.83	2.91	2.37	2.25
K_2O	1.71	1.74	1.90	1.71	1.50	1.70	1.88	1.93	1.25	1.67	1.43	1.94	1.88	1.84	1.46	1.55
P_2O_5	0.54	0.54	0.61	0.51	0.53	0.52	0.57	0.71	0.54	0.52	0.41	0.60	0.57	0.56	0.43	0.63
L.O.I	0.01	0.45	1.01	-0.19	1.49	0.40	0.01	2.21	1.19	0.98	-0.13	1.94	0.20	-0.12	0.16	1.78
Total	99.66	99.35	99.75	99.50	100.16	99.51	99.45	99.97	99.45	100.05	99.08	99.61	100.20	99.41	99.79	99.88
Cr	226.54	302.06	359.33	312.81	381.16	315.74	257.87	132.34	291.75	326.70	247.66	255.14	224.38	233.32	337.79	238.17
Co	79.69	85.91	109.86	117.61	103.43	95.25	73.13	83.33	133.76	94.30	100.20	101.14	113.86	91.07	95.72	111.68
Ni	177.26	208.55	233.66	244.48	254.17	226.46	193.47	110.16	237.94	270.24	212.04	255.47	216.32	196.81	257.45	225.54
Cu	56.16	50.79	59.05	58.72	61.95	56.80	53.43	75.97	66.25	57.85	57.89	54.77	52.92	52.20	50.14	68.45
Zn	98.73	83.05	90.50	100.04	98.81	96.19	89.68	103.89	95.64	88.86	93.71	101.63	87.21	83.99	87.46	108.82
Rb	19.61	23.53	30.25	25.69	22.30	27.81	19.89	18.44	18.65	18.46	17.36	24.70	23.85	23.12	19.29	17.36
Sr	557.53	712.32	817.46	739.26	903.47	820.35	585.37	676.48	825.19	616.88	547.18	676.97	712.28	693.28	577.76	535.56
Y	26.46	26.95	33.07	34.19	35.67	33.48	22.74	38.97	31.79	29.75	24.53	33.44	30.58	29.30	26.58	34.55
Zr	172.57	193.81	237.93	229.86	230.58	226.51	136.41	234.70	182.27	169.20	126.85	206.63	183.16	173.45	138.09	214.90
Nb	30.75	35.10	43.74	36.72	30.26	35.72	27.69	56.16	45.20	35.16	18.52	42.20	23.25	30.83	23.02	52.40
Ba	282.35	278.06	310.09	279.33	298.30	278.18	281.62	419.82	312.47	306.00	244.44	461.18	321.28	309.02	282.97	352.92
La	22.71	21.54	24.98	22.99	23.89	23.14	21.88	33.30	24.14	22.61	18.35	28.89	24.41	23.75	19.39	29.61
Ce	46.59	43.70	50.29	47.75	47.06	47.79	45.18	68.24	49.44	47.17	38.65	56.58	50.49	48.91	39.60	59.76
Nd	22.74	21.90	24.45	23.27	22.86	22.99	22.39	32.29	22.70	20.54	18.57	25.58	23.02	23.37	19.10	29.51
Sm	5.35	5.00	5.45	5.32	5.06	5.07	4.97	6.75	4.97	4.81	4.24	5.75	5.22	5.03	4.46	6.41
Eu	1.74	1.67	1.67	1.58	1.64	1.59	1.72	2.16	1.69	1.58	1.45	1.80	1.68	1.68	1.48	1.96
Gd	5.91	5.67	6.36	5.84	6.01	5.97	5.35	8.05	5.71	5.39	4.75	6.23	5.72	5.77	4.78	7.74
Tb	0.75	0.73	0.80	0.78	0.79	0.75	0.70	1.06	0.78	0.69	0.61	0.85	0.75	0.78	0.65	0.59
Yb	2.27	2.03	2.27	2.33	2.21	2.30	2.13	3.01	2.33	2.30	1.97	2.66	2.34	2.35	2.11	2.61
Lu	0.25	0.21	0.24	0.25	0.24	0.26	0.24	0.40	0.28	0.23	0.22	0.31	0.25	0.26	0.21	0.25
Hf	3.74	3.99	4.32	4.17	3.98	4.25	3.88	5.69	4.13	3.86	3.25	4.88	4.38	4.24	3.42	3.79
Th	3.01	3.05	3.52	3.06	2.82	3.06	3.15	5.04	3.14	3.13	2.50	3.48	3.04	3.00	2.62	2.55
Sc	24.92	26.84	25.54	25.54	27.74	24.54	24.53	22.84	26.29	22.23	24.80	22.51	21.75	21.01	20.50	18.93

FeO* represents total iron

Mineral compositions were obtained from phenocrysts and microphenocrysts of the rock samples and listed in Table 1. The forsterite (Fo) contents of olivine in the Jungok basalts range from 66 to 84%. Olivine makes up 14.2 to 23.2% of the mode, and the grains vary widely in size. Phenocrysts have more Fo contents (84~77.2) compared to the microphenocrysts (79.7~66.9) in general. Plagioclase is the most dominant mineral phase and it comprises from 45.7 to 60.3% of the rock. The anorthite content (An) of plagioclase analyzed in this study shows ranges from An51 to An71. Clinopyroxene is generally occured as micro- phenocrysts which comprises 16.2 to 28.7% of the rock. Clinopyroxenes are Ti-rich augite with a relatively narrow range in CaO (21.3~22.5%) and Al_2O_3 (4.1~7.4%), but have a wide range in FeO (7.5~12.2%), MgO (8.0~13.3%) and TiO_2 (2.4~6.9%).

Major and Trace Element Composition

The analyzed samples have alkalic compositions and show relatively restricted range in chemical composition (Table 2), particularly in the major elements such as SiO_2 (46.8~48.7%), K_2O (1.3~1.9%), FeO (10.6~11.8%), Na_2O (2.1~2.9%) and CaO (7.4~8.9%). However, they span a wide range in MgO (6.4~10.7%). Whole rock chemical analyses of rocks from the study area indicate that the all rocks fall within the alkali olivine basalt field in an SiO_2 vs. Na_2O+K_2O diagram.

With decreasing MgO contents, Al_2O_3, TiO_2 and P_2O_5 contents increase, while CaO decrease (Fig. 2). As MgO contents decrease from 11 to about 6%, TiO_2 contents increase but FeO contents do not define a systematic trend. However, at less than 8% MgO, abundances of FeO decrease rapidely with decreasing MgO. SiO_2, Na_2O and K_2O contents do not show any systematic trend with MgO.

Variation of trace elements with increasing magmatic differentiation for the Jungok basalts are indexed with wt.% MgO and are shown in Fig. 3. Trace element variation ranges wider than those of major elements. Abundances of trace elements vary by about a factor of two or more with changing MgO contents. Compatible elements, Ni and Cr, decrease

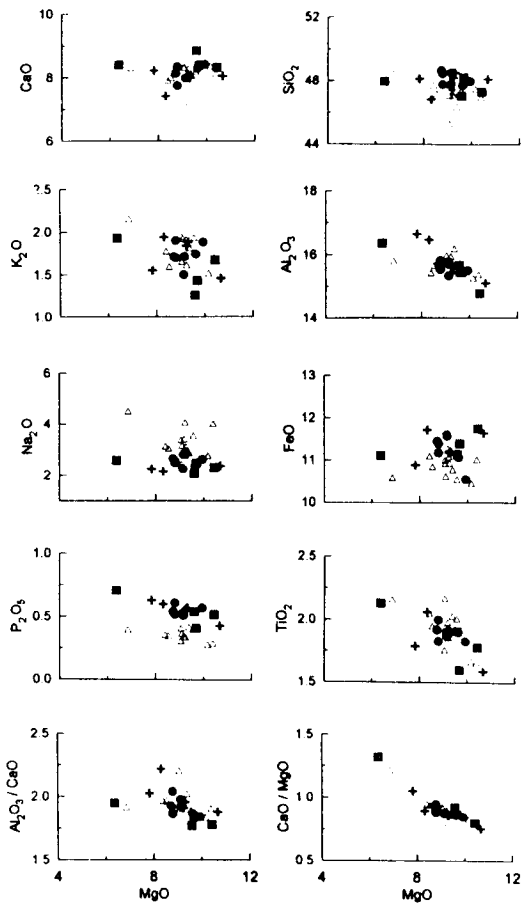

Fig. 2. Variation of major oxides as a function of MgO content in Jungok basalts. Data from this study and Won (1983). Symbols : filled circle; CB, filled square; CH, Cross; CO, open triangle; data from Won (1983).

with decreasing MgO, while the hygromagmatophile elements (Rb, Ba, Zr, Y, etc.) show a trend of enrichment with increasing differentiation. Plots of chondrite normalized (Thompson, 1982) REE data for the selected samples are shown in fig. 4. All samples have comparable abundances and degree of fractionation of REE. It show a typical alkali basalt REE pattern which is enriched in LREE compared HREE.

DISCUSSION

The chemical differentiation of most magmas results from processes operating in the subsurface.

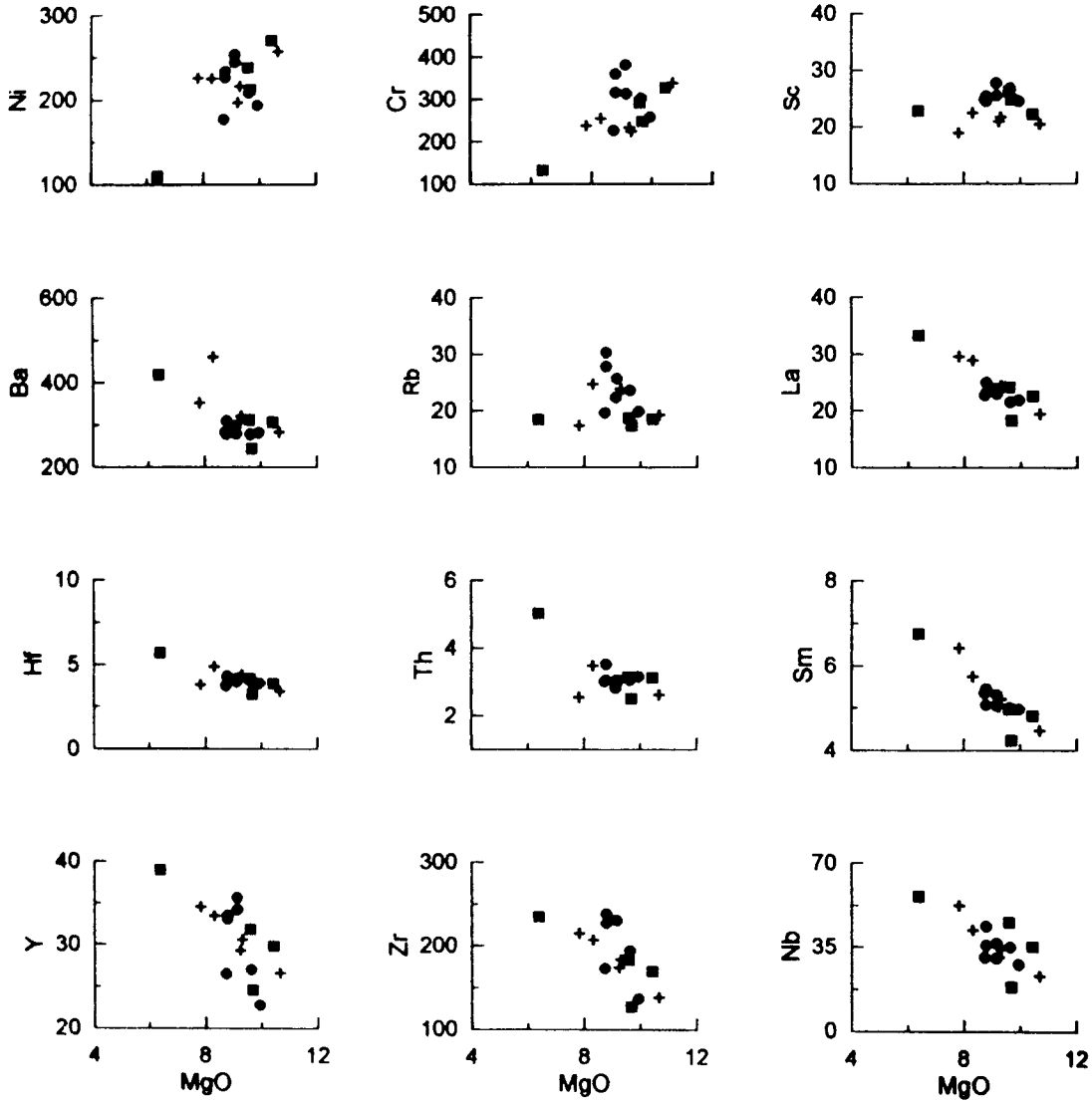

Fig. 3. Variation of trace elements as a function of MgO content in Jungok basalts. Symbols are same as in Fig. 2.

Factors responsible for the variation in chemistry of the Jungok basalts are likely to be some contribution of the following processes; crystal fractionation either with or without crustal assimilation, variation in degree of partial melting of the source during melt extraction, and a heterogeneous source on a small scale. Furthermore, the alteration effect also change the chemistry of the rocks.

In order to minimize the alteration effect on the chemistry of the studied rocks, the fresh rocks were selected for analysis on the basis of detailed petrographic study. Samples with amygdales, sericitized plagioclase, and altered groundmass were excluded. Thus, the role of alteration in the chemical variation of the rocks might be negligible in this study.

Evaluating the Role of Fractionation

If chemical diversity of the rocks are related by

crystal fractionation, the possible fractionating minerals are the phenocryst phases present in the less evolved basalt such as olivine, clinopyroxene and plagioclase. The change in slope on the MgO variation diagrams (Figs. 2, 3) is consistent with a major role for mineral/melt fractionation. Thus, increasing SiO_2, CaO/MgO ratio and decreasing Ni contents with decreasing MgO correspond to fractionation of a silica-poor, Mg-rich phase such as olivine. At the same time, increasing Al_2O_3/CaO ratio probably reflect clinopyroxene fractionation, and decreasing CaO contents are consistent with fractionation of plagioclase and/or clinopyroxene. The rapid decrease of FeO abundances with decreasing MgO for rocks containing less than 8% MgO probably indicates fractionation of phases enriched in FeO such as magnetite which occured as groundmass phase in the studied rock samples.

On the basis of partition coefficients between minerals and liquids, the falling values of Ni and Cr with decreasing MgO indicate fractionation of olivine and/or clinopyroxene. The rapid decrease in Sc content in samples with less than about 9% MgO might be suggest that a significant role for clinopyroxene and/or magnetite fractionation (partition coefficient of Sc for Cpx is 2.4 and Mgt is 3.1) at late stage. Trace element abundance ratios such as Ba/La, La/Yb, La/Eu, Nd/Sm, and Sr/Nd are sensitive to fractionation of mineral phases (Fig. 5). Decreasing Ba/La and Sr/Nd ratios with decreasing MgO contents require fractionation of plagioclase. Increasing La/Yb, La/Eu and Nd/Sm ratios with decreasing MgO may be due to fractionation of plagioclase and/or clinopyroxene. The narrow range of Zn contents indicates that the bulk partition coefficient between minerals and liquid is close to unity and is consistent with the combined fractionation of olivine,

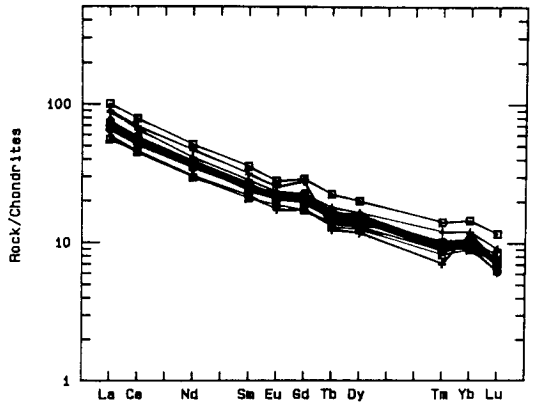

Fig. 4. Chondrite normalized REE patterns of Jungok basalt sample. Symbles : open circle; CB, open square; CH, cross; CO.

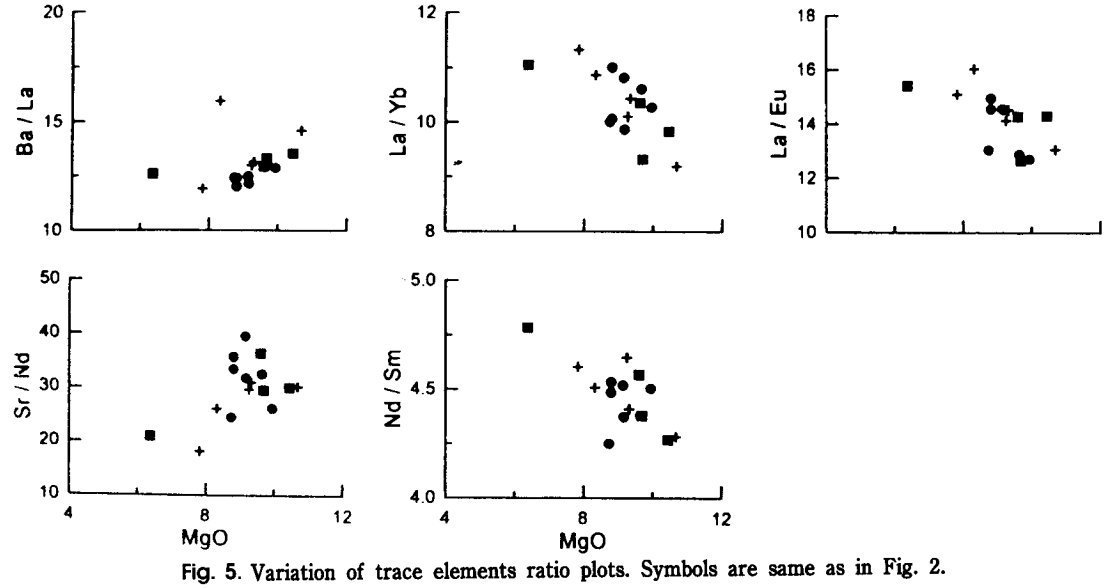

Fig. 5. Variation of trace elements ratio plots. Symbols are same as in Fig. 2.

Table 3. Fractionation calculations for presumed parent (CH-3) to evolved basalt (CH-1).

	SiO_2	TiO_2	Al_2O_3	FeO*	MnO	MgO	CaO	Na_2O	K_2O	P_2O_5	$SumR^2$
1. CH-3 = 78.42 CH-1 + 12.08 OL + 5.43 PLAG + 3.55 CPX + 0.52 MGT											
CH-1	49.07	2.18	16.74	11.36	0.15	6.51	8.60	2.65	1.97	0.73	
Calc.	49.05	2.08	16.66	11.44	0.07	6.56	8.68	2.67	2.11	0.66	
Diff.	-0.02	-0.10	-0.08	0.08	-0.08	0.05	0.08	0.02	0.14	-0.07	0.06
2. CH-3 = 81.53 CH-1 + 11.83 OL + 3.67 PLAG + 2.97 CPX											
CH-1	49.07	2.18	16.74	11.36	0.15	6.51	8.60	2.65	1.97	0.73	
Calc.	48.75	2.11	16.74	11.65	0.10	6.53	8.81	2.63	2.03	0.64	
Diff.	-0.32	-0.07	0.00	0.29	-0.05	0.02	0.21	-0.02	0.06	-0.09	0.25

All data normalized to 100% with water-free basis before calculation. FeO* represents total iron.
Mode 1 involves magnetite, model 2 does not.
OL; Olivine, PLAG; Plagioclase, CPX; Clinopyroxene, MGT; Magnetite.

clinopyroxene, plagioclase and Fe-Ti oxides (Clague *et al.*, 1981).

Fig. 4 shows the REE patterns of the studied rock samples, and none of these analyzed samples have negative Eu anomalies. Despite major and trace element evidences for plagioclase fractionation, Eu anomalies are absent in evolved rock samples. The Sr/Nd ratio, which is also a sensitive indicator of plagioclase fractionation, is not sensitive to oxygen fugacity (Chen *et al.*, 1990). Relative to the primitive basalts, evolved ones have lower Sr/Nd ratios (Fig. 5). It may suggest that the lack of negative Eu anomaly is due in part to the high oxygen fugacity of the lava which precluded significant reduction of Eu^{3+} to Eu^{2+} (Henderson, 1984).

Quantitative Modelling of Fractionation Processes

The evaluation of fractional crystallization is best performed on fresh rocks for which original mineral compositions are available. A fractional crystallization calculation was attempt to examine the possibility which produce the most evolved sample from the parent by removing solid phases. The evolution of the presumed parental rock to later compositions was modelled by multiple linear regression method (one involving magnetite in the crystallizing assemblage, the other not), then checked the trace element concentrations calculated by the model against those observed in the actual samples. In order to understand the compositional variations within the Jungok basalts, samples of CH-3 and CH-1 are used as endmembers. The modelling results show that the major element composition of daughter (CH-1) can be derived by; 1) fractionation of 12.1% olivine, 5.4% plagioclase, 3.6% clinopyroxene and minor amount (<1%) of magnetite, or 2) fractionation of 11.8% olivine, 3.7% plagioclase and 3% clinopyroxene from the presumed parent (CH-3). As mentioned previously, magnetite occured as groundmass phase

Table 4. Comparison of observed and calculated trace element compositions for magnetite-present model.

	obs. (CH-1)	calc.	calc./ obs.	Kds used in calculation			
				OL	CPX	PLAG	MGT
Rb	18.44	23.19	1.26	0.01	0.02	0.19	0.32
Sr	676.48	705.5	1.04	0.01	0.1	1.7	0.01
Ba	419.82	383.61	0.91	0.01	0.01	0.22	0.01
Zr	234.78	212.81	0.91	0.015	0.17	0.07	0.33
Sc	22.84	24.35	1.07	0.18	2.4	0.1	3.1
Co	83.38	79.37	0.95	1.4	1.7	0.04	4.61
Ni	110.16	93.21	0.85	10.0	2.0	0.01	5.0
Th	5.04	3.97	0.79	0.0002	0.026	0.05	0.19
Nb	56.16	44.57	0.79	0.005	0.05	0.01	0.4
La	33.3	28.62	0.86	0.0013	0.05	0.07	0.004
Ce	68.24	59.57	0.97	0.002	0.1	0.07	0.006
Nd	32.29	20.02	0.62	0.034	0.23	0.05	0.004
Hf	5.69	4.82	0.85	0.015	0.23	0.08	0.41
Sm	6.75	5.99	0.88	0.0058	0.44	0.03	0.006
Eu	2.16	1.94	0.90	0.0053	0.45	0.2	0.004
Yb	3.01	2.84	0.94	0.012	0.6	0.02	0.06
Lu	0.40	0.28	0.71	0.015	0.57	0.02	0.07

K_d; average of previously reported partition coefficients (Philpotts *et al.*, 1972; Arth, 1976; Cox *et al.*, 1978; Frey *et al.*, 1978; Clague *et al.*, 1981; McKay *et al.*, 1986; Wilson, 1988).

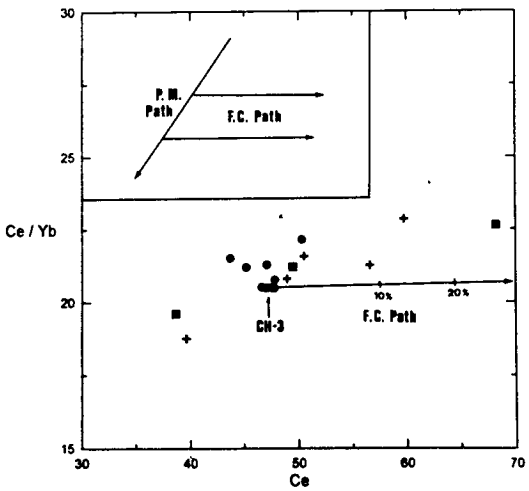

Fig. 6. Ce/Yb vs. Ce plot and schematic illustration showing evolutionary trends of fractional crystallization and partial melting processes. F.C.path represents fractional cystallization trend of fractionation of olivine, plagioclase, clinopyroxene and magnetite in the proportions 56 : 25 : 17 : 2. P.M.path represents schematic partial melting trend.

in some samples and magnetite fractionation may therefore have occured. The amount of fractionation calculated for the magnetite-free model (18.5%) is marginally smaller than in the magnetite-present model (21.6%), and the latter gives a better solution. The result of the calculations are presented in Table 3, and show a good fit between calculated and observed contents of major elements.

The mineral proportions estimated from major element modelling, and previously reported mineral/melt partition coefficients (Table 4) were used to calculate trace element abundances in the residual liquids. The calculation was carried out by using MAGMA-86 software developed by Hughes (1987). The calculated trace element abundances in the residual melts are compared to that in the proposed daughter and listed in Table 4. For the transition metals (Sc and Co), the calculated abundances in the residual liquids agree well with the measured abundances in the derived sample. For the incompatible elements, the calculated values are less than observed abundances in general. The major and compatible elements variation is consistent with fractional crystallization of plagioclase, clinopyroxene, olivine and magnetite. However, the calculated trace element abundances by fractional crystallization model underestimate the incompatible element concentrations in the evolved endmember.

Fig. 6 shows the Ce/Yb vs. Ce plot and fractional crystallization path with schematic illustration showing evolutionary trends of fractional crystallization and partial melting. As shown by fractional crystallization path in Figure 6, differentiation by fractional crystallization process alone seems to have difficulty evolving the observed Ce/Yb ratio and the Ce content in the sampled rocks. It suggest that the simple fractional crystallization process can not explain the chemical evolution of the Jungok basalts.

Possible Mechanisms for Enrichment of Incompatible Elements

One mechanism which could account for the larger than expected range of incompatible element concentration is varying degrees of partial melting of the source. Major and compatible trace elements would be buffered by the restite assemblage and show little change for degrees for melting less than about 15% (Harris *et al.*, 1990). However, only partial melting process can not account for the incompatible element abundances of the Jungok basalts. The Mg-number and Ni contents of the rocks are very low (Mg-no. : 36~48, Ni : 110~270 ppm) whereas magmas derived directly from the mantle should have Mg-numbers in the range 68~72 and 300~400 ppm Ni (Frey *et al.*, 1978). Thus, the low Mg-numbers and Ni contents in the samples indicate that the rocks were extensively fractionated prior to extrusion. In this case, the major element and compatible element variation is due to crystal fractionation, but the incompatible element variation is due to crystal fractionation superimposed on already varying concentrations, caused by slightly different degree of melting of the same source as shown by schematic illustration of the partial melting and fractional crystallization trends in Fig. 6.

Other alternative mechanism by which enrichment of incompatible trace elements can occure without

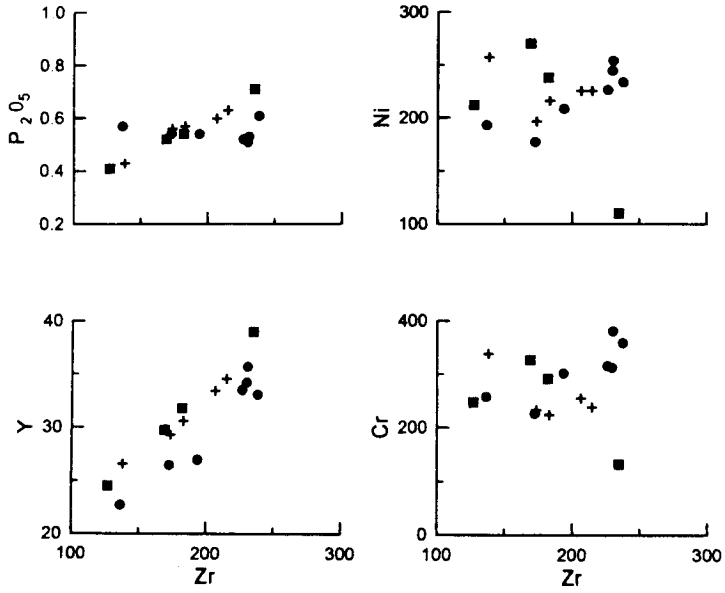

Fig. 7. Inter-element diagrams, P_2O_5, Y, Ni, and Cr vs. Zr for analysed samples from Jungok basalts. Symbols are same as in Fig. 2.

concomitant changes in major element composition is in a periodically replenishment, tapping, and crystal fractionation (RTF) magma chamber (O' Hara, 1977; O'Hara and Mathews, 1981; Chen *et al.*, 1990). With a constant replenishing magma composition and the operation of a large number of cycles of tapping and replenishment, a steady state is reached in which repeated cycles have a greater enrichment of incompatible elements than can be achieved by simple fractional crystallization (Chen *et al.*, 1990).

RTF type of magma evolution show a relatively good correlation between incompatible elements and the poor correlation between incompatible and compatible elements (Cox, 1988). Fig. 7 show a plots of Zr vs. compatible and incompatible elements. The incompatible elements P and Y show a strong correlation with Zr. On the other hand the correlation between Zr and the compatible elements Ni and Cr is very poor. These observations suggest that the possibility of RTF process can not be precluded to explain the magmatic evolution of the studied rocks. In the case of the Jungok basalts, if each replenishment cycles resulted in a lava flow then there should be at least eleven cycles between the lowest and the highest exposed flow. This number of cycle is sufficient for a steady state to be achieved in which incompatible element are enriched relative to major and compatible elements (Cox, 1988).

In summary, abundances of incompatible elements in the evolved rocks can not be explained by a simple crystal fractionation. The variation in incompatible element concentration may be due to magma batches being derived by slightly different degrees of partial melting, and/or periodic replenishment, tapping, and crystal fractionation processes.

CONCLUSION

Geochemical data indicate that the analysed samples are fall within the alkali olivine basalt field and show relatively restricted range in major element compositions except MgO. Chemical variation of the Jungok basalts can not explaind by simple fractional crystallization of olivine, clinopyroxene, plagioclase, and magnetite. The incompatible element data appear to require the other processes which enrichment of incompatible elements can occure without concomitant changes in major and compatible trace elements. Thus, in case

of the Jungok basalt, the major elements and compatible trace element variation is due to fractional crystallization, but the incompatible elements variation is probably due to fractional crystallization superimposed on already varying concentrations caused by slightly different degree of melting of the same source, and/or due to periodic replenishment, tapping and fractionation processes.

ACKNOWLEDGEMENT

Grateful acknowledge is made to S. C. Lee and S. K. Lee for their help in field study and sample preparations. Also, I am grateful to the Center for Mineral Resources Research for financial support.

REFERENCES

Arth, J.G. (1976) The behavior of trace elements during magmatic processes: A summary of theoretical models and their applications. J. Res. US Geol. Surv., v. 4, p. 41-47.

Chen, C.Y., Frey, F.A. and Gracia, M.O. (1990) Evolution of alkalic lavas at Haleakala Volcano, east Maui, Hawaii. Contrib. Mineral. Petrol., v. 105, p. 197-218.

Choi, M.C. (1982) Report of the third excavation in Cheon-kok Paleolithic site. J. Liber. Art., Kon-kuk Univ., v. 14, p. 207-238.

Clague, D.A., Frey, F.A., Thompson, G. and Rindge, S. (1981) Minor and trace element geochemistry of volcanic rocks dredged from the Galapagos spreading center: Role of crystal fractionation and mantle heterogeneity. J. Geophy. Res., v. 86, p. 9469-9481.

Cox, K.G. (1988) Numerical modelling of a randomized RTF magma chamber: A comparison with continental flood basalt sequences. J. Petrol., v. 29, p. 681-697.

Cox, K.G., Bell, J.D. and Pankhurst, R.J. (1978) The interpretation of igneous rocks. George Allen & Unwin, London, pp. 450.

Frey, F.A., Green, D.H. and Roy, S.D. (1978) Integrated models of basalt petrogenesis: A study of quartz tholeiites to olivine melilitites from southeastern Australia utilizing geochemical and experimental petrological data. J. Petrol., v. 19, p. 463-513.

Harris, C., Marsh, J.S., Duncan, A.R. and Erlank, A.J. (1990) The petrogenesis of the Kirwan basalts of Dronning Maud Land, Antarctica. J. Petrol., v. 31, p. 341-369.

Henderson, P. (1984) Rare earth element geochemistry. Elsevier Sci. Pub. New York, pp. 510.

Hughes, S.S. (1987) Geochemical modelling software. HUGUES Magmatics, Corvallis, Oregon.

Kim, K.H., Kim, O.J., Min, K.D. and Lee, Y.S. (1984) Structural, paleomagnetic and petrological studies of the Chugaryeong rift valley. J. Korean Inst. Mining Geol., v. 17, p. 215-230.

Lee, D.S. (1981) Volcanic activity in the southwest part of Choogaryong rift valley, Korea. Abstr. IAVCEI Symposium- Arc Volcanism.

Lee, D.S., Ryu, K.J. and Kim, G.H. (1983) Geotectonic Interpretation of Choogaryong Rift Valley, Korea. J. Geol. Soc. Korea. v. 19, no. 1, 19-38

McKay, G.A., Wagstaff, J. and Yang, S.R. (1986) Zirconium, hafnium, and rare earth element partition coefficients for ilmenite and other minerals in high-Ti lunar mare basalts: An experimental study. J. Geophy. Res., v. 91, p. D229-D237.

O'Hara, M.J. (1977) Geochemical evolution during fractional crystallization of periodically refilled magma chamber. Nature, v. 266, p. 503-507.

O'Hara, M.J. and Mathews, R.E. (1981) Geochemical evolution in an advancing, periodically replenished, periodically tapped, continuously fractionated magma chamber. J. Geol. Soc. London, v. 138, p. 237-277.

Philpotts, J.A., Schnetzler, C.C. and Thomas, H.H. (1972) Petrogenetic implications of some new geochemical data on ecologite and ultrabasic intrusions. Geochim. Cosmochim. Acta, v. 36, p. 1131-1166.

Takahasi, E. (1962) The Chukaryong rift line. Sci. Rep. Yamaguchi Univ., v. 13, p. 33-36.

Thompson, R.N. (1982) Magmatism of the British Tertiary Volcanic Province. Scottish J. Geol., v. 18, p. 1-108.

Ueda, N. (1968) Evolution of the continent in Northeastern Asia, I: Reconnaissance survey of the geochronology of the Korean Peninsula. unpublished M.S. Thesis, Tokyo Univ.

Wilson, M. (1988) Igneous petrogenesis. Unwin Hyman, London, pp. 466.

Won, J.K. (1983) A study on the Quaternary volcanism in the Korean Peninsula. J. Geol. Soc. Korea, v. 19, p. 159-168.

Manuscript received 13 February 1996

추가령 열곡대에 분포하는 전곡현무암의 지화학적 특성

위 수 민

요 약 : 제 4기 전곡현무암은 추가령 열곡대내의 한탄강유로를 따라 길게 분포하고 있으며 이대성 외 (1983)에 의하면 대략 10~20 m정도의 두께를 가지고 있다. 전곡현무암의 암석분화 과정을 밝히기 위해 57개의 시료가 채취되었으며, 이중 16개의 시료에 대한 주성분 및 미량원소의 화학분석이 실시되었다. 분석된 시료들의 화학조성에 의하면 전곡현무암은 알칼리계열의 현무암으로 특징지워지며, MgO를 제외한 주성분원소의 변화범위가 미량원소에 비하여 상당히 좁은 영역을 나타낸다. 분별결정작용 모델을 정량적으로 시험하기 위해서 Multiple linear regression을 사용하였다. 주성분원소와 반정으로 산출되는 광물의 화학조성을 사용하여 계산된 결과는 전곡현무암의 화학조성의 변화는 감람석, 사장석, 휘석, 자철석이 56 : 25 : 17 : 2의 비율로 분별정출되어 분화된 것으로 설명할 수 있다. 그러나 위의 결과를 가지고 미량원소의 함량을 계산하면 불호정 (incompatible) 원소의 계산치는 딸암석의 실제 함량에 미치지 못한다. 이러한 점으로 미루어 전곡현무암의 화학조성의 변화는 광물들의 단순한 분별정출 작용만으로는 설명하기가 어렵다. 따라서 전곡현무암의 화학조성의 변화는 약간 다른 정도의 부분용융에 의해 불호정원소의 초기치가 다른 것들이 분별정출과정을 겪었거나, 혹은 RTF과정에 의한 불호정원소의 부화가능성을 배제할 수 없음을 시사한다.